



HAL
open science

Preparation and Characterization of Glued Corn Flakes-Like Protein-Based Magnetic Particles

Waisudin Badri, Mohamad Tarhini, Zineb Lgourna, Nouredine Lebaz, Hassan Saadaoui, Nadia Zine, Abdelhamid Errachid, Abdelhamid Elaissari

► **To cite this version:**

Waisudin Badri, Mohamad Tarhini, Zineb Lgourna, Nouredine Lebaz, Hassan Saadaoui, et al.. Preparation and Characterization of Glued Corn Flakes-Like Protein-Based Magnetic Particles. Chemistry Africa, 2020, 3, pp.803-811. 10.1007/s42250-020-00147-2 . hal-02623651

HAL Id: hal-02623651


<https://hal.science/hal-02623651>

Submitted on 13 Nov 2023

HAL is a multi-disciplinary open access archive for the deposit and dissemination of scientific research documents, whether they are published or not. The documents may come from teaching and research institutions in France or abroad, or from public or private research centers.

L'archive ouverte pluridisciplinaire **HAL**, est destinée au dépôt et à la diffusion de documents scientifiques de niveau recherche, publiés ou non, émanant des établissements d'enseignement et de recherche français ou étrangers, des laboratoires publics ou privés.

Preparation and Characterization of Glued Corn Flakes-Like Protein-Based Magnetic Particles

Waisudin Badri¹  Mohamad Tarhini¹ · Zineb Lgourna² · Nouredine Lebaz¹ · Hassan Saadaoui³ · Nadia Zine⁴ · Abdelhamid Errachid⁴ · Abdelhamid Elaissari¹

Abstract

Purpose The aim of this study was to prepare and to characterize bovine serum albumin protein-based magnetic nanoparticles in terms of chemical composition (weight loss of organic material), physicochemical and colloidal properties.

Methods Bovine serum albumin-based iron oxide colloidal particles were prepared by coprecipitation of ferrous chloride (FeCl₂), ferric chloride (FeCl₃) in highly basic medium and in the presence of protein at high temperature. The particle morphology was examined using both Transmission Electron Microscopy (TEM) and Atomic Force Microscopy (AFM) whereas particle size, size distribution and zeta potential were obtained by Dynamic Light Scattering (DLS). The organic matter mass loading was revealed by Thermogravimetric Analysis (TGA).

Results The particle size was found to be submicronic, which confers to such magnetic colloids a low sedimentation rate. Their morphology was non-spherical and non-smooth in nature but glued corn flakes-like, which reflects the heterocoagulation mechanism process involved in the formation of the particles. The designed particles contain about 73% w/w iron oxide, whereas only 50% w/w was determined by magnetization.

Conclusion Proteins as promising crosslinking agents to prepare hybrid particles.

Keywords Hybrid particles · Protein · Crosslinking · Magnetic nanoparticles · Particle size · Size distribution

1 Introduction

Based on new estimations, 10% (more than US\$40 billion/year) or over 100 approved peptide-based therapeutics of the pharmaceutical market are peptide and protein drugs. Peptides and proteins (i.e., enzymes and antibodies) are highly selective thanks to their multiple target contacts in compare to the typical small drug molecules, which form

the large part of the pharmaceutical market [1]. Different types of proteins were employed like building blocks in the delivery of small molecules that attract much attention thanks to their unique properties including biocompatibility, biofunctionality, and biodegradability. Indeed, proteins such as gelatin, albumin, gliadin, zein could transport drugs over the blood brain barrier [2]. Nanoparticles are one of the largest groups of nanocarriers, have an important role in diagnostics and therapy [3]. Adequate characterization of nanoparticles (NPs) is very important in order to design well-defined nanoformulations of therapeutic relevance. Indeed, nanoparticle physicochemical properties contribute towards their behavior in the biological environment [4].

These nanoparticles are responsive to the magnetic field from the external environment and may be oriented and stimulated magnetically [3]. Magnetic particles have been used in numerous applications and especially in the biomedical area [5]. In biomedical diagnostics, magnetic particles are used as biomolecules carriers [6]. The first application of magnetic particles was in immunoassays in order to replace the heaviness of the centrifugation step when latexes are

✉ Waisudin Badri
waisudin.badri@univ-lyon1.fr

¹ University of Lyon, University Claude Bernard Lyon-1, CNRSLAGEPP-UMR 5007, 43 Boulevard du 11 Novembre 1918, 69100 Villeurbanne, France

² Labomine Laboratory, Lot No. 35, Ibnou Rochd, Z.I Tassila, 80000 Agadir, Morocco

³ Centre de Recherche Paul Pascal, Université de Bordeaux, 33600 Pessac, France

⁴ UMR 5280, Institut Des Sciences Analytiques, University of Lyon, CNRS, University Claude Bernard Lyon 1, 5 Rue de la Doua, 69100 Villeurbanne, France

used. Then, various applications have been reported such as controlled drug delivery (cancer, gene, and cardiovascular therapies), hyperthermia, tissue engineering, in specific affinity separation, cells isolation and sorting, biomolecules purification, nucleic acid extraction, purification and concentration, specific capture of DNA and RNA and also as contrast agents in Magnetic Resonance Imaging (MRI) [3, 7, 8]. These applications have been investigated using various manufactured colloidal magnetic particles. In addition, magnetic nanoparticles can be modified through ligands that are specific to the target organ or tissues receptor sites [3]. It is still crucial but challenging to prepare magnetic particles with the specifications imposed by the targeted application such as quality with well controlled size, a good size distribution and a high saturation magnetization [9]. Generally, the obtained particles are polydisperse in nature and in some cases, the presence of both magnetic and non-magnetic particles was not excluded.

Various academic research works devoted to the preparation of hybrid magnetic particles have been also reported. In this direction, special attention was dedicated to the preparation of multi stimuli-responsive particles such as thermally sensitive hybrid magnetic. The first work in this field has been reported by Kondo et al. [10]. This work is focused on the preparation of poly(styrene/*N* isopropylacrylamide/methacrylic acid) magnetic particles. The obtained hybrid particles are found to be polydisperse with low magnetic content.

Polystyrene core with magnetic shell hybrid particles have been prepared via heterocoagulation process as first reported by Furusawa et al. [11]. The encapsulation of electrostatically adsorbed iron oxide nanoparticles onto polystyrene seed was performed using various recipes based on emulsion polymerization of styrene in order to avoid the release of iron oxide. Unfortunately, the final hybrid particles release iron oxide nanoparticles during storage. This original process has been extended by Sauzedde et al. [12] through performing the adsorption of iron oxide nanoparticles onto the oppositely charged polystyrene-core/crosslinked poly(*N*-isopropylacrylamide)-core-shell followed by the encapsulation process via seed radical polymerization [13].

In order to prepare biocompatible magnetic hybrid particles and to avoid multi-steps preparation processes, special attention has been dedicated to the use of natural polymers in the formulation processes [3]. Natural polymers are used in recent years as coating matrices since they are capable of increasing the stability and the biocompatibility of magnetic nanoparticles. Xie et al. [14] developed a dopamine-plus-HSA (human serum albumin) approach to modify iron oxide nanoparticles for the labeling of various cell types in a nonspecific manner. Their efficiency was demonstrated by *in-vivo* magnetic resonance imaging on xenograft and focal cerebral ischemia models. More recently, Nosrati

et al. prepared bovine serum albumin (BSA)-coated magnetic nanoparticles as curcumin carriers through desolvation and chemical co-precipitation process [15]. The structural, colloidal and magnetic properties of the BSA-coated Fe₃O₄ nanoparticles loaded with curcumin were characterized and their cytotoxicity against breast cancer cells was investigated. Instead of using BSA, Chang et al. employed human-like collagen (HLC) protein as a coating material and explored the size and surface effects of the HLC-coated magnetic nanoparticles on the magnetic hyperthermia heating characteristics [16]. It has been shown that HLC coating enhanced the specific absorption rate (SAR) of the HLC-nanoparticles significantly and improved the biocompatibility of the nanoparticles. Khramtsov et al. functionalized the nanoclusters of carbon-coated iron nanoparticles with four different proteins including BSA, casein and two types of gelatins for application in biosensing [17]. They demonstrated that the protein-coated magnetic nanoparticles maintain their size in complex media such as juice, milk, serum and plasma and at elevated temperatures. This facilitates their application in homogeneous assays of biomarkers and foodborne pathogens and their applicability may be extended to *in-vivo* diagnostics and numerous medical applications as reported by Bealer et al. [18].

It is worth mentioning that the colloidal properties of particles (organic, inorganic and composite, etc.) are a crucial challenge facing especially users of magnetic colloids in biomedical applications. In fact, only the colloidal characterization of a given dispersion could help the preparation process, the optimization of biological assays and the particles integration in biological processes (i.e. nanotechnologies-based microsystems, *in-vivo* circulation of particles, etc.). In addition, the complete colloidal characterization of a prepared dispersion reveals the preparation quality and in some cases the synthesis mechanism. Then, before any application of colloidal particles, the dispersion and the particles require to be characterized in terms of size and size distribution, surface charge density, surface polarity, morphology, electrokinetic properties and colloidal stability. To some extent, all these properties are part of a systematic investigation in colloids science in which particles are generally used as a model colloid, a solid support for biomolecules, and/or a label for revealing the capture of targeted biomolecules.

In this work, to tackle this challenge, we focused on the complete characterization of the prepared BSA-iron oxide colloidal particles concerning particle size and size distribution, morphology, chemical composition, electrokinetic properties, magnetic properties (i.e. magnetic content and saturation magnetization) and colloidal stability.

2 Experimental

2.1 Materials

Ferrous chloride (FeCl₂), ferric chloride (FeCl₃), hydrochloric acid, ammonia, BSA protein and phosphate buffer were supplied by Sigma-Aldrich (Germany). Deionized Milli-Q water was used in all experiments as the dispersion medium.

2.2 Preparation of BSA-Based Iron Oxide Colloidal Particles

BSA-based iron oxide colloidal particles were prepared according to the well-known precipitation-crosslinking process. The precipitation was due to the reaction of FeCl₂ and FeCl₃ in highly basic medium and the crosslinking and the coating were induced by BSA at the preparation temperature (i.e. 70 °C). The crude magnetic dispersion was sorted (via sedimentation and magnetic separation) in order to obtain narrow size distributed magnetic particles.

The synthesis of ferrofluid was carried out at 20 °C in a thermostatically controlled reactor of 500 mL (without cover) equipped with a mechanical stirring system composed from an anchor with three branches. FeCl₂ and FeCl₃ were firstly dissolved in hydrochloric acid (1 M).

Once the dissolution of iron salts has completed (orange-colored homogeneous solution), concentrated ammonia (20%) was rapidly added into the reactor under strong agitation (1000 round per minute). The immediate appearance of a black precipitate corresponds to the ferrous oxide formation. The coprecipitation reaction was continued in the ammoniacal medium during one hour (the pH of reaction media was consequently near to 9). The particles were washed after decantation and finally redispersed in water to obtain a stable ferrofluid.

Prepared BSA in a 10⁻² M phosphate buffer was consecutively added directly in the reactor. One hour after, the reaction media was heated up to 70 °C. Then the mixture was placed on the magnetic agitation plate for two hours. The covered iron oxide nanoparticles by the dispersed BSA in the aqueous phase were collected after first sedimentation process, by the application of a permanent magnetic field using strong magnet and the precipitate was removed.

2.3 Characterization

2.3.1 Hydrodynamic Particle Size Analysis

Hydrodynamic particle size was measured by Quasi-Elastic Light Scattering (QELS) using the Zetasizer 3000HS from Malvern Instrument (Malvern, UK). The hydrodynamic

diameter of a highly diluted magnetic dispersion in 1 mM NaCl was measured. The colloidal stability was investigated by measuring the particle size as a function of salt concentration after 10 min incubation. The samples were prepared using deionized Milli-Q water. The mean hydrodynamic diameter D_h was then calculated from the diffusion coefficient measurement using the Stokes–Einstein equation:

$$D = \frac{kT}{3\pi\eta D_h} \quad (1)$$

where D is the diffusion coefficient, k the Boltzmann constant, T the absolute temperature, and η the dynamic viscosity of the medium. The particle size and size distribution were determined using Contin analysis mode.

2.3.2 Transmission Electron Microscopy

Transmission electron microscopy (TEM) was carried out using a Hitachi electron microscope (Hitachi S 800, CME-ABG at Claude Bernard University Lyon 1, France). The particles morphology was examined depositing one droplet of magnetic dispersion on TEM grid and then dried before analysis.

2.3.3 Electrophoretic Mobility Measurement

The electrophoretic mobility of the prepared dispersions was measured using the ZetaSizer 3000HS, from Malvern Instruments. The experiments were carried out using highly diluted dispersions in aqueous 1 mM NaCl solution or in 1 mM phosphate buffer solution at pH = 6. The electrophoretic mobility was determined as a function of pH (at a constant ionic strength) and as a function of salt concentration at a stable pH (1 mM phosphate buffer, pH 6). In this study, the electrophoretic mobility (μ_e) values were converted to the zeta potential (ζ) using the classical Smoluchowski's Eq. (2)

$$\mu_e = \frac{\epsilon_0 \epsilon_r \zeta}{\eta} \quad (2)$$

Where ϵ_0 and ϵ_r are the permittivity of vacuum and relative permittivity of the medium respectively.

All the measurements were at least the average of triplicate values and performed at 25 °C.

2.3.4 Thermogravimetric Analysis (TGA)

To determine chemical composition, thermogravimetric analysis was used. An Atomic Emission Spectrometer equipped with the Plasma and inductive coupling or Inductively Coupled Plasma (ICP), was used to determine the amount of organic and inorganic materials forming the prepared BSA-based magnetic particles. Measurements were

performed under nitrogen atmosphere for about 10 mg of samples in a dried state between 25 °C and 550 °C at a heating rate of 10 °C/min (TGA from AT Instruments).

2.3.5 Magnetic Properties (Saturation Magnetization)

The saturation magnetization (M_s) and magnetic behavior of the dried BSA-magnetic particles were investigated using a vibrating sample magnetometer. This study was carried out on the Automatic Bench of magnetic measurements, CNRS-IRC Lyon. Magnetization of dried particles was investigated by increasing the magnetic field (H) from zero to + 21,000 Oersted at room temperature.

3 Results and Discussion

3.1 Composition

The organic content of the magnetic material was deduced by thermogravimetric (TGA) measurements performed under nitrogen with a heating rate of 10 °C/min until 550 °C. Weight loss occurring under 550 °C can be attributed to the BSA fixed at the particles surface. Then, the non-calcinated material can be considered as residual inorganic material and corresponds to iron oxide. The amount of inorganic material was found to be about 73% w/w as deduced from the weight loss as a function of temperature illustrated in Fig. 1. It is worth mentioning that the analysis was performed on BSA-based iron oxide dispersion after total removal of both BSA molecules and primary magnetic nanoparticles.

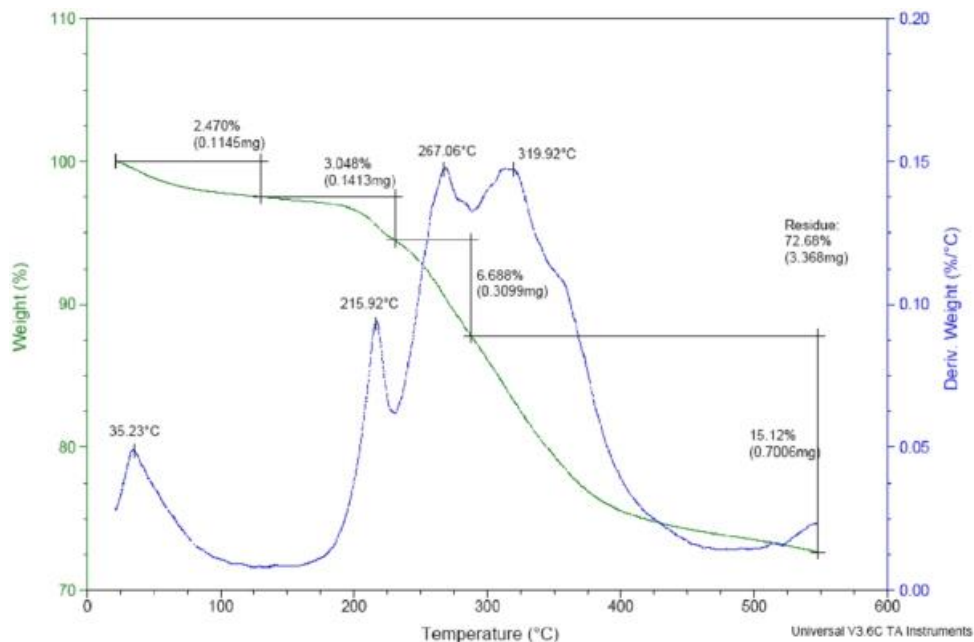
3.2 Particle Size and Size Distribution

The size and size distribution of magnetic particles are critical, especially in the case of medical applications. For instance, Wang et al. pointed out the impact of superparamagnetic nanoparticle size on the performance of lateral flow immunoassay [19]. Hence, to tune the size of BSA-coated nanoclusters, variations in pH could be applied [20]. Protein-coated nanoparticles are sensitive to sonication. This parameter may be used for nanoparticle size manipulation as reported by Sangeetha and Philip [21] and Khramstov et al. [17].

In the case of our study, hydrodynamic particle size and size distribution of highly diluted dispersions were examined using dynamic light scattering. The average hydrodynamic diameter was found to be around 140 nm \pm 20 nm, with a narrow size distribution ranging from 100 to 175 nm as reported in Fig. 2. Since the hydrodynamic particles size is below 900 nm, no sedimentation was observed even after few days' storage.

As clearly shown from light scattering analysis, the obtained hydrodynamic particle size is larger than the size of individual primary iron oxide magnetic particles which is in between 8 and 12 nm [22]. This result explains basically the formation of submicron clusters. If individual particles of iron oxide are coated by adsorbed BSA, the particles size should be not far from the hydrodynamic size of individual particles except in the presence of some aggregated particles as reported by Nosrati et al. [23]. In fact, by using BSA for individual iron oxide magnetic nanoparticles coating, they obtained particles of around 56 \pm 11 nm. However, this mean size is calculated by image processing based on TEM

Fig. 1 Thermogram of dried BSA-based magnetic particles obtained by TGA analysis



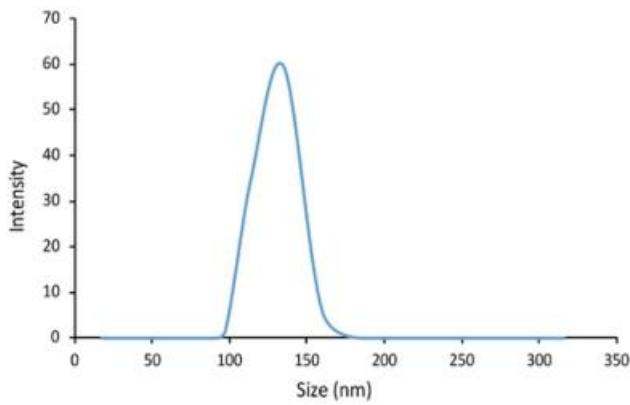


Fig. 2 Hydrodynamic particle size and size distribution of the prepared BSA-based magnetic particles in 1 mM NaCl at 25 °C obtained by dynamic light scattering measurement

micrographs (and not by light scattering) showing particles overlapping which makes their analysis tricky [15]. Functionalized nanoclusters of carbon-coated iron magnetic nanoparticles with BSA were prepared following the protocol described by Mikhalev et al. [17, 24]. They obtained nanoclusters whose mean sizes is ranging from 114 to 233 nm in the different tested cases. These results are via adsorption at room temperature and not via BSA crosslinking process at high temperature. Consequently, even if the reported sizes are in agreement with the mean diameter obtained in our study which is around 145 nm, the preparation processes conditions are different [20].

3.3 Electrokinetic Study

Surface charge affects the stability of the protein-based magnetic particles and their behavior when dispersed in a given biological fluid such as blood for example. The interactions between the particles themselves and between the particles and biological entities (cells, proteins, etc.) will be affected by the nature of the surface charge of the particles, the particles surface charge density and the surface polarity [25]. It is then crucial to determine the electrokinetic properties of the magnetic nanoparticles in different conditions of pH and salinity, which mimic the properties of the intended application media.

The electrophoretic mobility (μ_e) of the prepared BSA-based magnetic particles was first measured as a function of pH in a 1 mM NaCl buffer at 25 °C. The obtained values were converted into zeta potential using Eq. (2). The zeta potential values of highly diluted BSA-based magnetic particles as a function of pH and at a constant ionic strength (1 mM NaCl) are presented in Fig. 3. The zeta potential values are found to be positive at acidic pH until pH 6 and then negative above pH 6. The positive zeta potential can be attributed to the protonation of amine groups and the

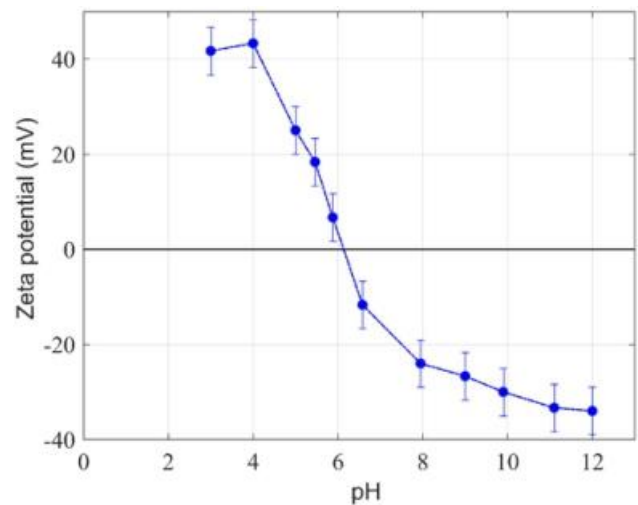


Fig. 3 Zeta potential of the BSA-coated magnetic particles versus pH in 1 mM NaCl, at 25 °C

negative one can be attributed to the dissociation of carboxylic group. Such zeta potential profile was induced by the BSA molecules rather than the surface charges on primary iron oxide nanoparticles. In fact, BSA molecules are highly charged above and below pH 6.5. This isoelectrical pH (pH 6.5) of the formulated particles was found to be the same as for BSA molecules [26].

The high zeta potential values at acidic or basic pH should confer to prepared particles appreciable colloidal stability in the pH domain below pH 5 and above pH 7. The measured zeta potential at pH 6 reflects the low surface charge density. It is interesting to notice that no aggregation phenomenon was observed. The observed colloidal stability can be attributed to hydration forces induced by the protein shell [27].

Nosrati et al. obtained a zeta potential of -10.1 mV by analysing their BSA-coated magnetic particles loaded with curcumin in phosphate buffered (10 mM, pH 7.4) [15]. The observed difference in zeta potential can be attributed to the difference in salinity of the measurement medium and also to the non-crosslinking of BSA-coated magnetic particles reported by Nosrati et al. [23].

The zeta potential was also investigated as a function of salinity at a constant pH of 4.5 and the obtained results are reported in Fig. 4. The average zeta potential decreases as the ionic strength increases; this trend is theoretically expected. This is due to the changes in the slipping plan corresponding to the zeta potential induced by decreasing κ^{-1} (the Debye length) [13].

3.4 Colloidal Stability

Colloidal stability of any colloidal dispersion to be used for both in-vivo and in-vitro biomedical application is of

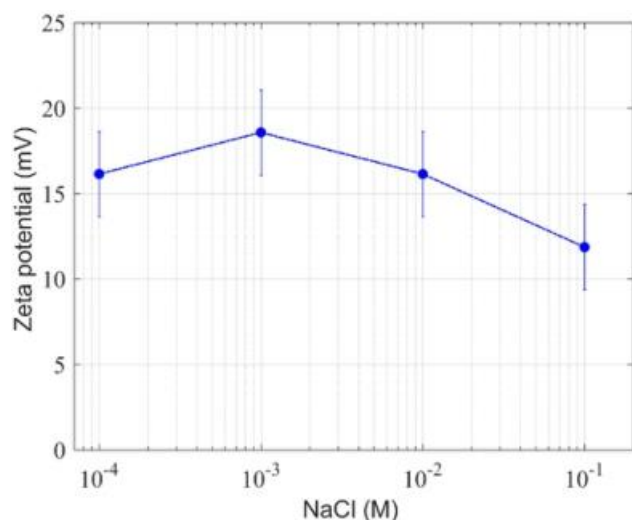


Fig. 4 Zeta potential of the prepared BSA-based magnetic particles versus NaCl concentration at pH 4.5 and at 25 °C

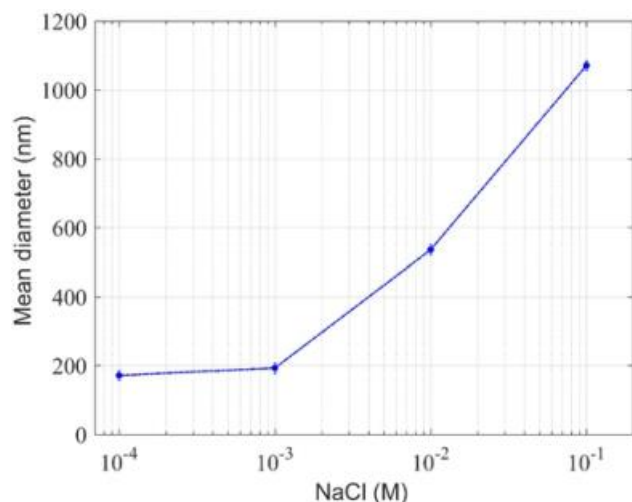


Fig. 5 Hydrodynamic particle size versus NaCl concentration in solution of pH 4.37, at 25 °C

paramount importance. Colloidal stability was examined by measuring the hydrodynamic particle size as a function of salt concentration at a constant pH of 4.37 and after 1 h storage. As clearly seen from Fig. 5, the aggregation phenomenon of magnetic particles appears above 10 mM salt concentration, which is encouraging principally for the majority of biomedical applications. The observed aggregation can be attributed to the screening of the repulsive electrostatic interactions between particles. Using such static colloidal stability methodology, the critical coagulation concentration, the Hamaker constant and the surface potential are not reachable experimentally as generally

reported for this new colloidal dispersion [28, 29]. In fact, the aggregation kinetic study should be considered.

The colloidal stability of such crosslinked protein-based magnetic particles has never been investigated. Whilst, the colloidal stability of polymer particles bearing adsorbed BSA has been investigated as reported by Molina-Bolivar et al. [30]. The reported results show that the hydration forces ensure the colloidal stability of the particles. This difference can be attributed to the nature of interfacial BSA molecules; in one case they are totally denaturated and crosslinked and the reported case, the BSA molecules are not folded and denaturated.

3.5 Surface Charge Density

The surface charge density of such particles cannot be determined using classical conductometry and pH titrations [31]. This is due to the possible titration of buried of comment chemical compounds such as carboxylic, amine, and hydroxyl groups. If we assume that the particles are perfectly coated with BSA molecules, the surface charge density is a combination of both amine and carboxylic groups. Consequently, the surface charge density can be estimated from the conversion of zeta potential to surface potential and then to surface charge density as reported for similar complex systems [28]. This gives in the case of our prepared crosslinked BSA-based magnetic particles a surface charge density in between -6.6 and $-7.5 \mu\text{C}/\text{cm}^2$ in a highly basic conditions (pH between 10 and 12). In this pH range, the amine groups are totally deprotonated and the measured zeta potential can be attributed to the dissociation of carboxylic groups only. Then the density of carboxylic groups on the formulated particles can be estimated to be above $-6.6 \mu\text{C}/\text{cm}^2$. Whereas, the surface charge density deduced from zeta potential determined below pH 4.0 can be attributed to the protonated amine only and was found to be around $+7.0 \mu\text{C}/\text{cm}^2$.

3.6 Morphology Analysis

The particles morphology was examined using various microscopic techniques such as transmission electron microscopy (TEM) and atomic force microscopy (AFM) in order to study the shape and the surface texture of the particles.

The particles shape was first examined using TEM and the obtained micrograph is presented in Fig. 6. Using such technique, to some extent, the particles can be considered spherically shaped as showed in a study performed by Talha et al. [32]. It is interesting to notice that using TEM to examine such small complex nanoparticles is problematic. To confirm the light scattering measurement, TEM was carried out. Surprisingly, the particles cannot be individually

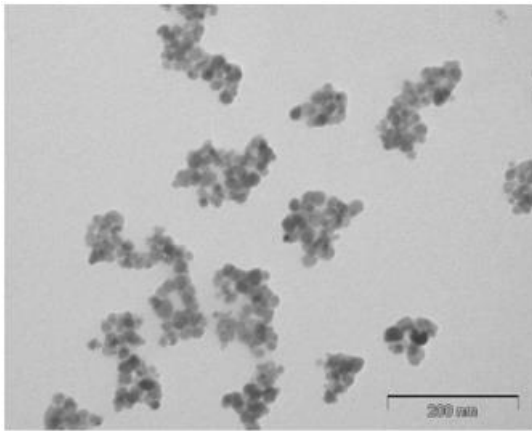


Fig. 6 Transmission electron micrograph of clustered magnetic nanoparticles

observed under appreciable resolution in order to determine the particle size as illustrated in the TEM micrograph. In addition, the sharpness of the viewed particles cannot be exactly defined. This observed behavior can be attributed to (i) low particle size of such particles and (ii) the presence of a protein shell around not only primary iron oxide nanoparticles but also the formed clusters. We can only deduce from the presented micrographs that the formulated BSA-based iron oxide particle size can't be considered as homogeneously size distributed (monodisperse) and cannot be considered as spherical particles. The observed separate clusters mean size is close to the one determined by light scattering. It is interesting to mention that BSA can be seen by TEM even under crosslinking state. In addition, possible flatness and fragmentation of the cluster and sample preparation of such clusters is questionable.

Atomic force measurements (AFM) were also performed in contact mode. The appearance of blobs smooth surface explains the presence of a homogeneous protein shell around the associated iron oxide nanoparticles, but the surface morphology of the cluster is not spherical and not smooth too. The BSA-based magnetic particles can be considered as an association of at least 10 blobs of 40 nm size as clearly evidenced by TEM (Fig. 6) and the particle size deduced from AFM (Z average, Fig. 7) is found to be in between 136 and 165 nm.

3.7 Magnetic Properties

Magnetic properties of BSA-based magnetic nanoparticles were examined using a classical magnetization method. The magnetization of nanoparticles was recorded in an applied magnetic field of $H(\text{Oe}) \leq 21,000$ at room temperature. Indeed, TGA and magnetization measurements are

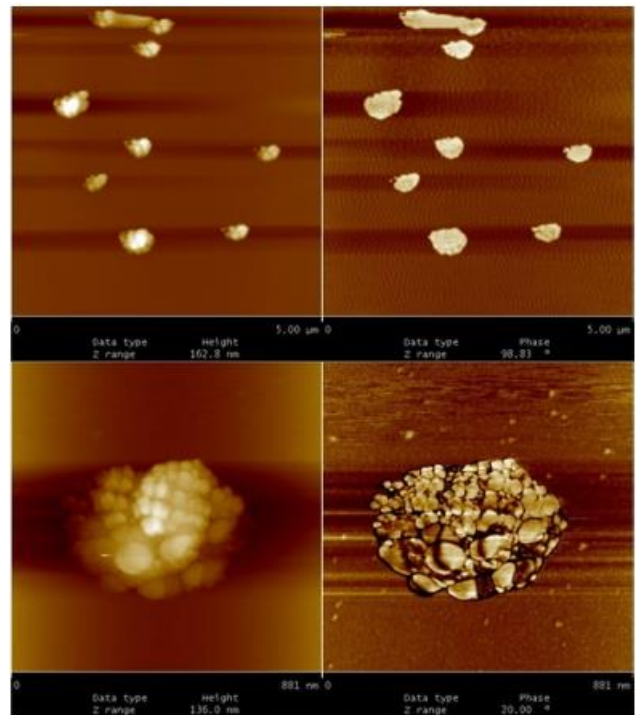


Fig. 7 Atomic Force Microscopy (AFM) images of BSA-based magnetic particles before (left) and after (right) image processing

complementary approaches to characterize the magnetic hybrid colloidal particles [33].

Firstly, the magnetization curve (Fig. 8) follows the Langevin function with no remanence (residual magnetization), which proves the superparamagnetic behavior of the magnetic material, which is an interesting property in various applications and principally in the biomedical

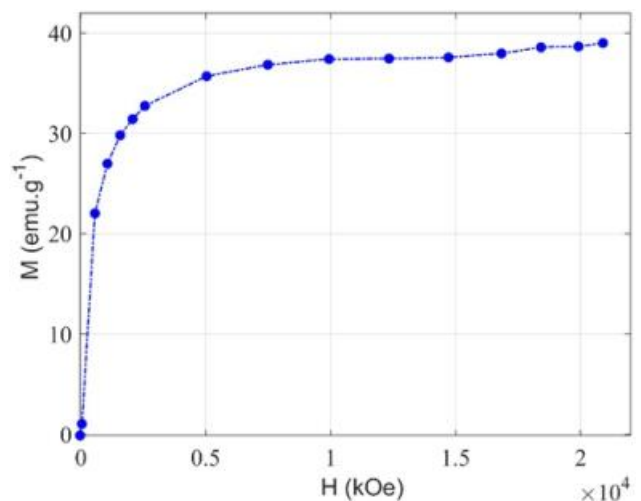


Fig. 8 Magnetization curve of the BSA-coated magnetic nanoparticles as a function of the applied field

field. The maximum magnetization deduced from the plateau value revealed the non-negligible magnetic properties of the particles since the magnetization at saturation is around 40 emu/g. Then, by assuming that such particles are principally from Fe₂O₃-based (79.6 emu/g) and by using the magnetization at the plateau value of BSA-based magnetic particles (40 emu/g), the amount of iron oxide material is found to be around 50% w/w. This value is lower than the chemical composition determined by TGA study (i.e. 73% w/w) as above discussed. This difference can be attributed to: (i) the presence of non-magnetic inorganic material such ferric and ferrous hydroxides and (ii) low magnetic Fe₃O₄ or gamma-Fe₂O₃ content in the composite particles. In fact, TGA is based on calcination of organic material and magnetization is based on the magnetic property of the used material (i.e. maghemite and magnetite).

Note that the maximum magnetization in our case is the same as that obtained by Nosrati et al. [23] for BSA-coated iron nanoparticles which was around 35 emu/g at a magnetic applied field of 104 Oe [15]. In the last study, the nanoparticles were loaded with curcumin which reduced further their magnetization. The reduction of the nanoparticles magnetization when coated with BSA is due to protein layer as explained by Maboudi et al. [34].

4 Conclusion

Structural, colloidal and magnetic properties of the formulated BSA protein-based iron oxide nanoparticles were characterized in this study after few fractionations. The particle size was found to be submicronic with a mean hydrodynamic diameter of around 145 nm. The particles morphology was investigated via TEM and AFM and found to be non-spherical but glued corn flakes-like morphology, which reflects the non-controllable heterocoagulation mechanism involved in the formation of the final particles. The colloidal stability of the prepared BSA-based particles prepared at high temperature is low compared to particles coated with BSA via adsorption at room temperature. This has been attributed to the protein crosslinked nature and denaturation in the case of high temperature. Regarding chemical composition, a high difference has been observed between TGA and magnetization results. In fact, TGA analysis revealed that the BSA-based iron oxide nanoparticles contain about 70% w/w iron oxide, whereas only 50% w/w was determined by magnetization. In addition, the prepared BSA-based iron oxide particles exhibited superparamagnetism, even if some of the magnetic properties are lost. Nevertheless, the residual magnetization is sufficient to be used in biomedical separation and drug targeting applications.

Acknowledgements The authors acknowledge Mr. Hassan Saadaoui from CRPP Bordeaux for his contribution in AFM analysis of this study.

Compliance with Ethical Standards

Conflict of interest The authors declare no conflict of interest.

References

1. Bruno BJ, Miller GD, Lim CS (2013) Basics and recent advances in peptide and protein drug delivery. *Ther Deliv* 4:1443–1467
2. Tarhini M, Pizzoccaro A, Benlyamani I, Rebaud C, Greige-Gerges H, Fessi H, Elaïssari A, Bentaher A (2020) Human serum albumin nanoparticles as nanovector carriers for proteins: application to the antibacterial proteins “neutrophil elastase” and “secretory leukocyte protease inhibitor”. *Int J Pharm* 579:119150
3. Denkbaş EB, Çelik E, Erdal E, Doğa K, Öznur A, Gökür K, Cem B (2016) In: Grumezescu AM (Grumezescu A) Magnetically based nanocarriers in drug delivery. *Nanobiomaterials in drug delivery*, 1st edn. William Andrew, Romania
4. Bhattacharjee S (2016) DLS and zeta potential—what they are and what they are not? *J Control Release* 235:337–351
5. Jamshaid T, Tenório-Neto ET, Eissa M, Zine N, El-Salehi AE, Kunita MH, Elaïssari A (2015) Preparation and characterization of submicron hybrid magnetic latex particles. *Polym Adv Technol* 26:1102–1108
6. Wu W, Wu Z, Yu T, Jiang C, Kim WS (2015) Recent progress on magnetic iron oxide nanoparticles: synthesis, surface functional strategies and biomedical applications. *Sci Technol Adv Mater* 16:023501
7. Mandrand B, Veyret R, Elaïssari A, Chatterjee J (2003) In colloidal biomolecules, biomaterials, and biomedical applications (Elaïssari A, Marcel D) biomedical application for magnetic latexes, 1st edn. CRC Press, Boca Raton
8. Cardoso VF, Francesko A, Ribeiro C, Bañobre-López M, Martins P, Lanceros-Mendez S (2018) Advances in magnetic nanoparticles for biomedical applications. *Adv Healthc Mater* 7:1700845
9. Xianyu Y, Wang Q, Chen Y (2018) Magnetic particles-enabled biosensors for point-of-care testing. *TrAC Trends Anal Chem* 106:213–224
10. Kondo A, Fukuda H (1997) Preparation of thermo-sensitive magnetic hydrogel microspheres and application to enzyme immobilization. *J Ferment Bioeng* 84:337–341
11. Sauzedde F, Elaïssari A, Pichot C (1999) Hydrophilic magnetic polymer latexes. 1. Adsorption of magnetic iron oxide nanoparticles onto various cationic latexes. *Colloid Polym Sci* 277:846–855
12. Sauzedde F, Elaïssari A, Pichot C (1999) Hydrophilic magnetic polymer latexes. 2. Encapsulation of adsorbed iron oxide nanoparticles. *Colloid Polym Sci* 277:1041–1050
13. Hunter RJ (1981) The calculation of zeta potential. In: *Zeta potential in colloid science*. Elsevier, New South Wales
14. Xie J, Wang J, Niu G, Huang J, Chen K, Li X, Chen X (2010) Human serum albumin coated iron oxide nanoparticles for efficient cell labeling. *Chem Commun* 46:433–435
15. Nosrati H, Sefidi N, Sharafi A, Danfar H, Manjili HK (2018) Bovine serum albumin (BSA) coated iron oxide magnetic nanoparticles as biocompatible carriers for curcumin-anticancer drug. *Bioorganic Chem* 76:501–509
16. Chang L, Liu XL, Fan DD, Miao YQ, Zahang H, Ma HP, Liu QY, Ma P, Xue WM, Luo YE, Fan HM (2016) The efficiency of magnetic hyperthermia and in vivo histocompatibility for human-like

-
- collagen protein-coated magnetic nanoparticles. *Int J Nanomed* 11:1175–1185
17. Khrantsov P, Barkina I, Kropaneva M, Bochkova M, Timganova V, Nechaev A, Byzov I, Zamorina S, Yermakov A, Rayev M (2019) Magnetic nanoclusters coated with albumin, casein, and gelatin: size tuning, relaxivity, stability, protein corona, and application in nuclear magnetic resonance immunoassay. *Nanomaterials* 9:1345
 18. Bealer EJ, Kavetsky K, Dutko S, Loflan S, Hu X (2020) Protein and polysaccharide-based magnetic composite materials for medical applications. *Int J Mol Sci* 21:186
 19. Wang Y, Xu H, Wei M, Gu H, Xu Q, Zhu W (2009) Study of superparamagnetic nanoparticles as labels in the quantitative lateral flow immunoassay. *Mater Sci Eng C* 29:714–718
 20. Khrantsov P, Kropaneva M, Byzov I, Minin A, Timganova V, Bochkova M, Uimin M, Zamorina S, Yermakov A, Rayev M (2019) Conjugation of carbon coated-iron nanoparticles with biomolecules for NMR-based assay. *Colloids Surf B Biointerfaces* 176:256–264
 21. Sangeetha J, Philip J (2012) The interaction, stability and response to an external stimulus of iron oxide nanoparticle–casein nanocomplexes. *Colloids Surf Physicochem Eng Asp* 406:52–60
 22. Montagne F, Mondain-Monval O, Pichot C, Mozzanaega H, Elaissari A (2002) Preparation and characterization of narrow sized (o/w) magnetic emulsion. *J Magn Magn Mater* 250:302–312
 23. Nosrati H, Sefidi N, Sharafi A, Danafar H, Manjili HK (2018) Bovine Serum Albumin (BSA) coated iron oxide magnetic nanoparticles as biocompatible carriers for curcumin-anticancer drug. *Bioorganic Chem* 76:501–509
 24. Mikhalev KN, Germov AY, Uimin MA, Yermakov AE, Konev AS, Novikov SI, Gaviko VS, Ponosov YS (2018) Magnetic state and phase composition of carbon-encapsulated Co@C nanoparticles according to ^{59}Co , ^{13}C NMR data and Raman spectroscopy. *Mater Res Express* 5:055033
 25. Clement JH, Schwalbe M, Buske N, Wagner K, Schnabelrauch M, Görnert P, Kliche KO, Pachmann K, Weitschies W, Höffken K (2006) Differential interaction of magnetic nanoparticles with tumor cells and peripheral blood cells. *J Cancer Res Clin Oncol* 132:287–292
 26. Bukackova M, Rusnok P, Marsalek R (2018) Mathematical methods in the calculation of the zeta potential of BSA. *J Solut Chem* 47:1942–1952
 27. Valle-Delgado JJ, Molina-Bolívar JA, Galisteo-González F, Gálvez-Ruiz MJ (2011) Evidence of hydration forces between proteins. *Curr Opin Colloid Interface Sci* 16:572–578
 28. Montagne F, Braconnot S, Mondain-Monval O, Pichot C, Elaïssari A (2003) Colloidal and physicochemical characterization of highly magnetic o/w magnetic emulsions. *J Dispers Sci Technol* 24:821–832
 29. Nabzar L, Duracher D, Elaïssari A, Chauveteau G, Pichot C (1998) Electrokinetic properties and colloidal stability of cationic amino-containing *N*-isopropylacrylamide-styrene copolymer particles bearing different shell structures. *Langmuir* 14:5062–5069
 30. Molina-Bolívar JA, Galisteo-González F, Hidalgo-Álvarez R (1997) Colloidal stability of protein-polymer systems: a possible explanation by hydration forces. *Phys Rev E* 55:4522–4530
 31. Elaïssari A, Lansalot M, Mondain-Monval O (2003) Colloidal biomolecules, biomaterials, and biomedical applications (Elaïssari A, Marcel D) colloidal polymers, 1st edn. CRC Press, Boca Raton
 32. Jamshaid T, Eissa MM, Lelong Q, Bonhommé A, Augsti G, Zine N, Errachid A, Elaïssari A (2017) Tailoring of carboxyl-decorated magnetic latex particles using seeded emulsion polymerization. *Polym Adv Technol* 28:1088–1096
 33. Tenório-Neto ET, Jamshaid T, Eissa M, Kunita MH, Zine N, Agusti G, Fessi H, El-Salhi AE, Elaïssari A (2015) TGA and magnetization measurements for determination of composition and polymer conversion of magnetic hybrid particles. *Polym Adv Technol* 26:1199–1208
 34. Maboudi SA, Shojaosadati SA, Arpanaei A (2017) Synthesis and characterization of multilayered nanobiohybrid magnetic particles for biomedical applications. *Mater Des* 115:317–324